



EISSN: 2788-9920
NTU Journal for Renewable Energy
Available online at:
<https://journals.ntu.edu.iq/index.php/NTU-JRE>



Effect of The Surface Pits on The Performance of a Double-Tube Heat Exchanger

Saba Reyad Alrefae¹, Adnan M. Alsaffawi², Younis M. Najim³

^{1,2,3}Department of Mechanical Engineering, College of Engineering, University of Mosul, Iraq

Article Informations

Received: 24 – 08 – 2025

Accepted: 02 – 11 - 2025

Published: 05 – 11 - 2025

Corresponding Author:

Saba Reyad Alrefae

Email:

seba.23enp72@student.uomosul.edu.iq

Key words: Double pipe heat exchanger, Rough surfaces, Heat transfer coefficient, The effectiveness of heat exchanger, Pits.

ABSTRACT

Heat exchangers are widely used to transfer heat between different fluids in various applications such as cooling systems, heating, and thermal industries. To improve the performance of these exchangers, several methods were used, including adding protrusions or indentations on the surface tube walls to increase fluid turbulence and enhance heat transfer. In this research, the effect of pits on the outer surface of the inner tube, with circular and square shapes arranged in linear and staggered patterns, on the performance of a double-tube heat exchanger with counterflow was studied. The flow of hot water inside the tube was fixed at 3.5 liters/minute at an inlet temperature of 50°C, while the flow of cold water was varied between 4.5 and 7.5 liters/minute at an inlet temperature of 22°C. The results showed that the presence of pits significantly improved thermal performance compared to the smooth tube. The improvement achieved in average Nusselt number is 24% for linear circular pits compared to the smooth tube, while it reached 31% for staggered circular pits. In case of square pits, the improvement achieved in average Nusselt number was 22% for linear arrangement, while it reached 30% for staggered arrangement. These results confirm that the use of pits, especially in a staggered arrangement, is an effective method for improving the performance of heat exchangers.



© THIS IS AN OPEN ACCESS ARTICLE UNDER THE CC BY LICENSE. <http://creativecommons.org/licenses/by/4.0/>

Introduction

Heat exchangers are considered one of the most important means of heat transfer in many industrial and domestic applications. They are used in power generation plants of all types (steam, gas, hydraulic, and others), as well as in cooling and air-conditioning systems, in addition to various other applications. In order to enhance the thermal performance of heat exchangers, researchers have employed various methods, such as using nanomaterial to improve the thermal conductivity of the fluids used, or adding extended surfaces on the tube surface of the heat exchanger or roughen the surface of the exchanger tube with different ways to increase the area for heat transfer and obtain turbulent flow of the fluids passing the exchanger. These techniques have led to improved thermal and mechanical properties of heat exchanger systems, thereby increasing their overall efficiency and leading to lower energy consumption [1]. Many researchers have conducted various studies on heat exchangers. Firstly, in a numerical study conducted by Malapur et. al. [2], by making spherical dimples on the outer surface of the inner tube, inclined at different angles and arranged in a spiral pattern. The outer diameter of the inner tube was 141.28 mm and had a thickness of 15.06 mm, while the outer tube had an inner diameter of 250 mm. The length of the heat exchanger was 1500 mm. Hot water flowed inside the inner tube at an inlet temperature of 67°C, while cold water flowed through the annular space at an inlet temperature of 25°C. The findings showed that the presence of dimples on the tube surface significantly increased the heat transfer coefficient compared to a smooth tube. Farsad et. al. [3], conducted a numerical study on a heat exchanger. Its inner tube contains concave and convex spherical dimples, as shown in Figure(1). A computational fluid dynamics (CFD) was used to analyze the performance of the system. The results showed an enhancement of 36.21% in the rate of heat transfer when the dimpled tube was used compared to the smooth tube exchanger. Also, the findings revealed that the dimples caused an increase in the Reynolds number which led to an increase in friction coefficient at a rate ranging between 6% to 25%. Asok et al. [4], performed a numerical study on a double-tube heat exchanger, whose inner tube surface contains rectangular and triangular annular cavities. The flow rate of hot and cold water used were 0.4 kg/s and 0.8 kg/s respectively. ANSYS FLUENT software was used for simulation analysis. The results indicated that the thermal performance for rectangular cavities better than that of triangular one. Also, Ali and Shehab [5], complete a numerical investigation on the performance of a heat exchanger with a dimpled inner

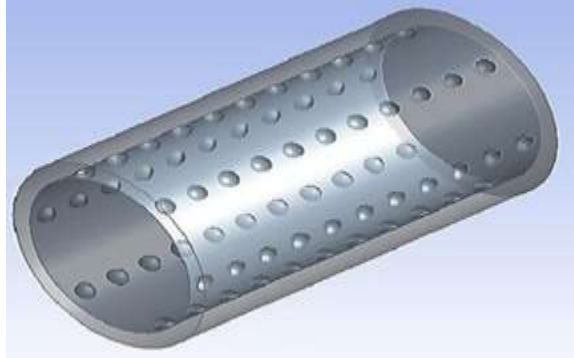
tube surface. The dimples are spherical and arranged linear and offset patterns.



Figure(1) Concave and convex spherical dimples [2].

They utilized a(CFD), specifically the k- ϵ model. The effects of arrangement, distribution angle, and distance between dimples were examined at various Reynolds numbers. The findings showed an enhancement in Nusselt number reached 50% with offset arrangement compared to linear, at a distribution angle of 60 degrees, Reynolds number of $Re = 10000$, and a distance between dimples of 8 mm. In addition, Ali et al. [6], done a numerical analysis of heat transfer in a double-tube heat exchanger, where the outer surface of the inner tube contained dimples arranged in two different patterns: linear and staggered, with varying distances between the dimples. The analysis focused on studying the effects of dimple arrangement and spacing on heat transfer performance. The results showed a 50% improvement in the Nusselt number for tubes with staggered dimples compared to those with linear arrangements. The thermal performance factor, which measures the efficiency of heat transfer enhancement relative to the flow resistance (pressure drop), ranged between 1.67 and 5.22 for the linear arrangement, while it ranged from 4.91 to 8.63 for the staggered arrangement. Furthermore, the highest performance factor of 9.07 was achieved with dimples of 6 mm in diameter, a spacing of 8 mm between the dimples, and a Reynolds number of 10,000 in the staggered arrangement. Cheng et al. [7], conducted a numerical study focusing on the effect of various factors on the heat transfer rate and performance of a heat exchanger. The researchers used a heat exchanger with a corrugated inner tube featuring spiral joints in different shapes. Water was used as a working fluid in the exchanger tubes. The results showed that decreasing the angle of inclination of the spiral corrugation from 28.42° to 10.81° led to an approximately 20% increase in the heat transfer coefficient. Similarly, Mohammed et. al. [8], conducted a numerical investigation to know the effect of hemispherical dimples, shown in Figure(2), on heat transfer and fluid flow with in the double-tube heat

exchanger, with the Reynolds number ranging from 6,000 to 14,000. A significant improvement of 17.3% in heat transfer rate was obtained compared with a smooth tube heat exchanger. Also, they found that larger dimples provided better thermal and hydraulic performance.



Figure(2) The hemispherical dimples on the outer surface of the inner tube of the heat exchanger [8].

Furthermore, a computational fluid dynamics (CFD) method, specifically the $k-\epsilon$ model, was used in a numerical study performed by Ghashim[9], on a double-tube heat exchanger. The inner tube contains dimples with different shapes (circular, square, and diamond). The number of Reynolds (Re) ranged from 2,500 to 15,000. The results indicated that the presence of dimples on the surface of tube enhances the heat transfer rate. For circular dimples of diameters 4 mm, 6 mm, and 8 mm, the Nusselt number was higher than that of smoother surface by 22%, 28%, and 43% respectively. Also, he found that circular dimples achieved the highest rate of heat transfer and low friction coefficient compared to other dimple shapes. Zhang et al.[10], study a numerically the effect of depth oval dimples on the hydraulic and thermal performance a tube-type heat exchanger. the (CFD) of $k-\epsilon$ model was used with Reynolds number ranging from 10,000 to 40,000. The findings showed that increasing the dimple depth from 1 mm to 2 mm led to a 30.47% increase in the Nusselt number and a 64.12% increase in the friction coefficient. In addition, Al-Haidari et al.[11], conducted a numerical and experimental study on a double-tube heat exchanger, where the outer surface of the inner tube was equipped with dimples and compared to a smooth tube. The simulation was performed using the Reynolds-Averaged Navier-Stokes (RANS) equations and the $k-\epsilon$ turbulence model, within a Reynolds number range of 4,000 to 15,000. The results showed an increase in the heat transfer rate in tubes with dimples, particularly at a Reynolds number of 6,000. Additionally, the numerical simulation results were

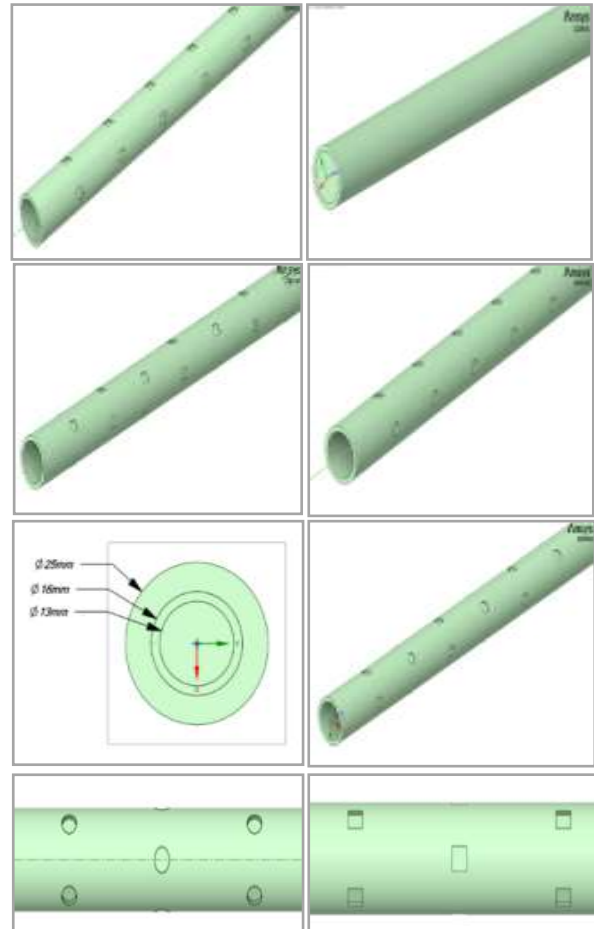
found to be very close to the experimental data, though slight discrepancies were observed in the predictions of heat transfer and pressure drop, with errors of approximately 6.7% and 9.4%, respectively. Similarly, In a numerical analysis conducted by Ali et al.[12], on the thermal-hydraulic performance of water flow in a tube with grooves of different shapes (square, circular, and triangular), the Reynolds number ranged from 3,500 to 7,000. A computational fluid dynamics (CFD) model, specifically the $k-\epsilon$ turbulence model, was used for the simulation. The numerical results showed that the grooved tube surface enhances the heat transfer rate and increases the friction coefficient compared to a smooth tube. The increase in the Nusselt number was approximately 12.808%, 17.987%, and 20.978% for square, circular, and triangular grooves, respectively. Moreover, Wantha et. al.[13], conducted a study focused on enhancing heat transfer in a double-tube heat exchanger, featuring a smooth inner tube and a dimpled outer tube. They utilized a nanofluid composed of water and aluminum oxide (Al_2O_3), which flowed through the space between the two tubes at different volumetric concentrations of aluminum oxide particles (0.1%, 0.6%, 1%, and 2%). The results showed that the Nusselt number increased by 4.7%, 12.0%, 28.8%, and 32%, respectively, leading to an improvement in the heat exchanger's performance. Additionally, In a numerical and experimental study conducted by Hussein and Freegah[14], on double-tube heat exchanger, various types of fins were examined. These included longitudinal fins, discontinuous longitudinal fins, and helical fins inclined at different angles (180° , 270° , and 90°), with a constant heat flux of 8000 W/m^2 applied to the inner surface of the inner tube. The researchers used the ANSYS Fluent program for the numerical analysis of the models, calculating the Nusselt number (Nu), pressure drop, and thermal resistance. The results were verified by manufacturing two models: the traditional model and the optimal model (Model D) based on the numerical study. The experimental results showed good agreement with the numerical analysis, and it was found that the eight semi-spiralfins with angle of 90° achieved the best performance, with a 66.76% improvement in heat transfer and a 47.1% reduction in thermal resistance. Similarly, Marzouk et al.[15], conducted a numerical and experimental study to enhance heat transfer in a double-tube heat exchanger by attaching screws to the outer surface of the inner tube. Each screw had a length of 17 mm and a diameter of 2.5 mm. Three different screw-to-screw distances were tested: 25 mm, 50 mm, and 100 mm. The length of the heat exchanger was 1 meter, with an inner diameter of 19 mm for the inner tube and an inner diameter of 5 mm for the outer tube. The flow was turbulent, with the Reynolds number ranging from

5700 to 3200. The experimental and theoretical results showed good agreement. It was observed that the highest improvement in heat transfer rate, 128%, occurred when the distance between screws was 25 mm. In a numerical study conducted by Alhulaifi, the focus was on the flow properties and convective heat transfer of nanofluids composed of water and titanium oxide (TiO_2) at volumetric concentrations of 0.2%, 0.4%, and 0.6%, with a Reynolds number ranging from 4,000 to 18,000. The results showed that the convective heat transfer coefficient of the nanofluid increased by 1.94% compared to pure water. Additionally, it was observed that the heat transfer coefficient increased with increasing Reynolds number. In another numerical study conducted by Somanchi et al. on a double-tube heat exchanger, nanofluids composed of TiO_2 and SiC in water at different volumetric flow rates of the cold fluid, ranging from 17.5 to 34.5 liters per minute, while maintaining a constant mass flow rate of the hot fluid. The results indicated that using a nanofluid composed of TiO_2 -SiC and water, with a nanoparticle mixing ratio of TiO_2 :SiC = 1:2, achieved the best thermal performance. The total heat transfer rate and friction factor increased by 11.20% and 22.92%, respectively [16].

1. Physical Modal

This study investigates the effect of surface pits on the performance of a counterflow double-tube heat exchanger. The heat exchanger consists of an inner tube made of aluminum, with an inner diameter of 13 mm and an outer diameter of 16 mm. The outer diameter of the shell (inner tube) is 25 mm, and the length of the heat exchanger is 1m. The flow of hot water inside the tube was fixed at 3.5 liters/minute at a temperature of 50°C, while the flow of cold water was varied between 4.5 and 7.5 liters/minute at an inlet temperature of 22°C. The study focuses on the effect of pits made on the inner surface of the tube. Two types of pits were used: square and circular, with two different arrangements: linear and staggered. These pit shapes and arrangements are shown in **Figure(3)**. The depth of the pits in both shapes is set to 1 mm, maintaining an identical surface area for the square and circular shapes. Since the properties of the fluid (water) change with temperature, this variation was considered in the calculations, meaning that the properties of water were not constant but varied according to the temperature variation. It was assumed that the flow inside the tubes is turbulent, based on the high velocities of the fluid. To analyze the results and determine the effect of the pits on the thermal performance of the heat exchanger, numerical

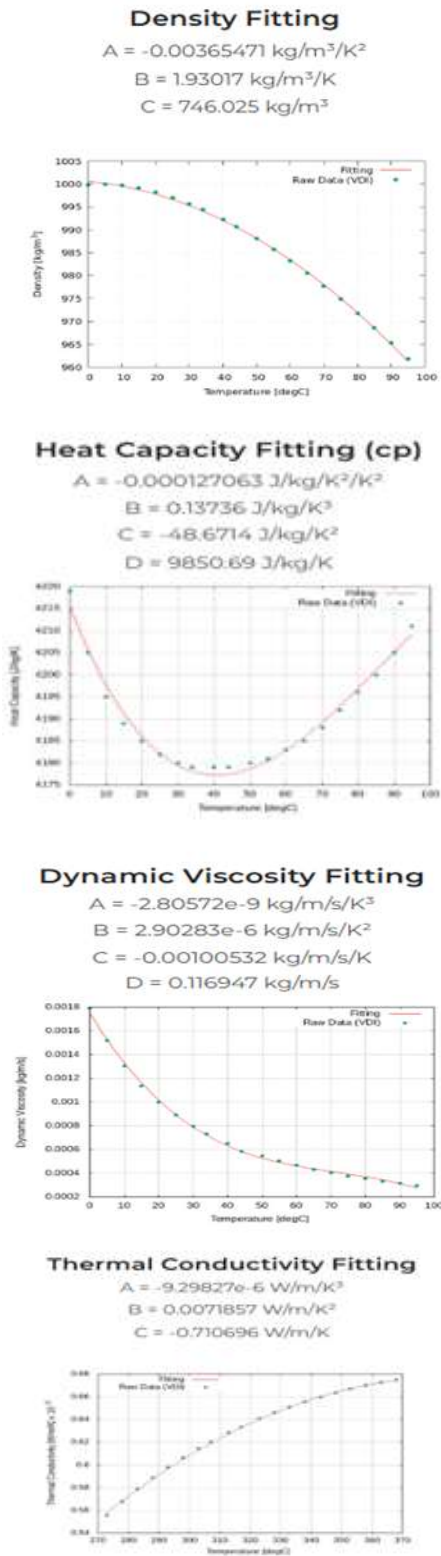
simulations were conducted using ANSYS Fluent. These simulations help to study the impact of pit arrangement (linear and staggered) and pit shape (square and circular) on improving heat exchange efficiency within the heat exchanger.



Figure(3) Schematic diagram illustrating the different types and arrangements of pits on the inner surface of the heat exchanger tube. The pits are of two shapes: elliptical and circular, with two distinct arrangements: linear and staggered. The pit depth for both shapes is 1 mm, ensuring identical surface area for both shapes.

1.1 Physical properties of water as a function of temperature

This research relied on variable thermal properties of water that depend on temperature instead of using constant values, in order to increase accuracy. Equations describing the changes in density, specific heat, conductivity, and viscosity with temperature were introduced. is shown in Figure(4).



Figure(4) Variation of water properties with temperature.

1.2 Governing Equations

- Continuity equation[17]:

$$\frac{\partial \rho u}{\partial x} + \frac{\partial \rho v}{\partial y} + \frac{\partial \rho w}{\partial z} = 0 \dots\dots(1)$$

where ρ is the density, and u, v and w are the velocities in the x, y and z .

- Moment equation[17]:

$$\frac{u}{\partial x} \frac{\partial \rho u}{\partial x} + \frac{v}{\partial y} \frac{\partial \rho u}{\partial y} + \frac{w}{\partial z} \frac{\partial \rho u}{\partial z} = \frac{-\partial p}{\partial x} + \frac{\partial}{\partial x} \frac{\mu}{\partial x} \frac{\partial u}{\partial x} + \frac{\partial}{\partial y} \frac{\mu}{\partial y} \frac{\partial u}{\partial y} + \frac{\partial}{\partial z} \frac{\mu}{\partial z} \frac{\partial u}{\partial z} \dots\dots\dots(2)$$

$$\frac{u}{\partial x} \frac{\partial \rho v}{\partial x} + \frac{v}{\partial y} \frac{\partial \rho v}{\partial y} + \frac{w}{\partial z} \frac{\partial \rho v}{\partial z} = \frac{-\partial p}{\partial y} + \frac{\partial}{\partial x} \frac{\mu}{\partial x} \frac{\partial v}{\partial x} + \frac{\partial}{\partial y} \frac{\mu}{\partial y} \frac{\partial v}{\partial y} + \frac{\partial}{\partial z} \frac{\mu}{\partial z} \frac{\partial v}{\partial z} \dots\dots\dots(3)$$

$$\frac{u}{\partial x} \frac{\partial \rho w}{\partial x} + \frac{v}{\partial y} \frac{\partial \rho w}{\partial y} + \frac{w}{\partial z} \frac{\partial \rho w}{\partial z} = \frac{-\partial p}{\partial z} + \frac{\partial}{\partial x} \frac{\mu}{\partial x} \frac{\partial w}{\partial x} + \frac{\partial}{\partial y} \frac{\mu}{\partial y} \frac{\partial w}{\partial y} + \frac{\partial}{\partial z} \frac{\mu}{\partial z} \frac{\partial w}{\partial z} \dots\dots\dots(4)$$

Where p is the pressure and μ is the viscosity.

- Energy equation[17]:

$$\frac{u}{\partial x} \frac{\partial T}{\partial x} + \frac{v}{\partial y} \frac{\partial T}{\partial y} + \frac{w}{\partial z} \frac{\partial T}{\partial z} = \frac{\partial}{\partial x} \frac{\alpha}{\partial x} \frac{\partial T}{\partial x} + \frac{\partial}{\partial y} \frac{\alpha}{\partial y} \frac{\partial T}{\partial y} + \frac{\partial}{\partial z} \frac{\alpha}{\partial z} \frac{\partial T}{\partial z} \dots\dots\dots(5)$$

Where α is the thermal diffusivity.

- Solid side[17]:

$$\frac{\partial^2 T}{\partial x^2} + \frac{\partial^2 T}{\partial y^2} + \frac{\partial^2 T}{\partial z^2} = 0 \dots\dots(6)$$

1.3 Boundary Conditions

For the numerical analysis, the following assumptions were imposed.

- 1.The flow was steady and three-dimensional.
- 2.Radiation heat transfer was negligible.
3. The properties of water are variable and not constant.
4. All velocity components are zero at the walls (no-slip condition) hence: $u=v=w=0$.
5. The Standard $k-\epsilon$ turbulence model was adopted to simulate the turbulent flow inside the heat exchanger.
6. $RE = \frac{\rho u d}{\mu} \dots\dots\dots(7)$
7. The coefficient of heat transfer is defined as :

$$h_x = \frac{q''}{T_{wall(x)} - T_{bulk(x)}} \dots\dots\dots(8)$$

The amount of convective heat transport is measured by the Nusselt number. The Nusselt number is described

As:

$$Nu = \frac{h_x}{k_d} \dots\dots\dots(9)$$

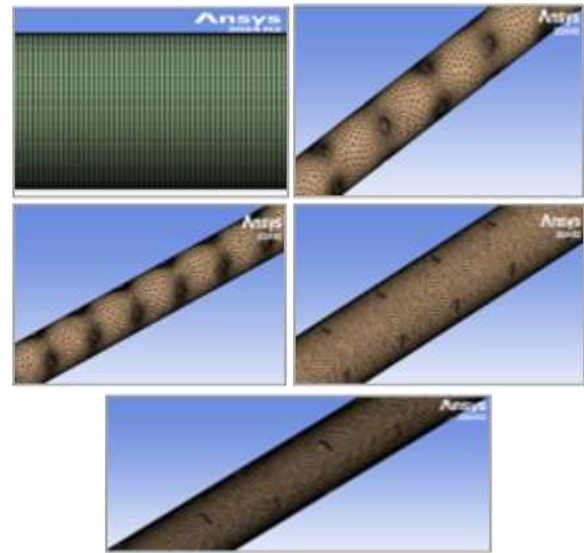
1.4 Mesh Study

After completing the geometric design of the heat exchanger, a numerical mesh was created covering the three domains: the liquid domain, the solid domain, as shown in the Figure(5), and the shell domain, with the aim of achieving a balance between result accuracy and numerical computation efficiency. For the liquid domain, a multi-region mesh was used,

and inflation layers were applied near the inner walls to ensure accurate representation of the boundary layer and the thermal changes resulting from the interaction between the liquid and the surface. In the solid domain, a mesh was created using an appropriate element size to represent the thermal gradients within the solid body while maintaining efficiency. In the shell domain, inflation layers were added to enhance heat transfer representation in the areas in contact with the liquid. This network setup provides a strong foundation for analyzing flow behavior and heat transfer within the heat exchanger, and is an essential step in conducting a Mesh Independence Study to ensure the reliability of the numerical simulation results using CFD. The Network Autonomy Study is an important step in computational fluid dynamics (CFD) to ensure accurate results from simulation without incurring excessive computational costs. This study aims to analyze the effect of the number of lattice elements on the Nusselt number, which is an important indicator of the performance of heat transfer by convection inside the heat exchanger. The graph shows the change of the Nusselt number with the difference in network density. At low-resolution networks — specifically at about 1,474,457 elements - Nusselts figure was approximately 21.6, indicating that the thermal gradients and flow distribution were not solved accurately enough. As the grid improved to 2,037,136 elements, the Nusselt number increased, demonstrating improved thermal behavior representation. When the number of elements increased to 2,309,225, the Nusselt figure reached about 22.9, a very small change compared to the previous level. This small change confirms that the solution has reached a stage of network independence, where additional increases in the number of elements do not have a tangible impact on the results. These results show that coarse meshes underestimate the number of Nusselt, This leads to inaccurate thermal predictions, while accurate networks give more reliable results but at the expense of greater computational time and resources. Thus, an element count of approximately 2.3 million is the best for striking a balance between the accuracy of the results and the efficiency of the computational performance, ensuring reliable predictions of heat transfer performance in the heat exchanger. Figure.1. shows the mes independence for the heat exchanger.

Table1. Effect of mesh resolution on Nusselt number

Grid Elements	Nusselt number
1433212	21.6258
1443785	22.4657
1456092	22.5025
1505897	22.6397
1567525	22.7529
1975767	22.8501
2484821	22.9024
3574036	22.9087



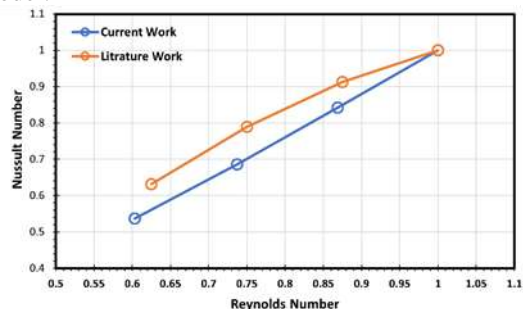
Figure(5) A three-dimensional computational mesh for the simulations.

2. Result and Discussion

2.1 Numerical validation

To verify the accuracy of the numerical model used in this study, a comparison was made between the current numerical results and a previous study published in the [5] ,which addressed the thermal performance of a double-pipe heat exchanger of the counterflow type, with dimples of different geometric shapes on the outer surface of the inner tube. The relationship between the Nusselt number and the Reynolds number was represented in both studies, where the reference study relied on a Reynolds number range of 5000 to 8000, while it ranged from 2509 to 4141 in the current study. To achieve an accurate comparison, the numerical values of the results were normalized. The curve of the relationship between Nusselt number and Reynolds number showed a converging behavior between the two studies, with the Nusselt number increasing as the Reynolds number increased in both cases. This reflects the expected improvement in heat transfer as a result of increased flow velocity accompanied by turbulence in the fluid. This upward trend reflects the correct physical behavior of heat transfer by convection within the heat exchanger. The mean absolute percentage error (MAPE) between the results of the two studies was approximately 9.8%, which is an acceptable rate that confirms the accuracy of the numerical model used and its reliability in representing thermal performance under the studied conditions. These results indicate that the numerical model is capable of simulating the actual thermal behavior of the studied heat exchanger, and it is a

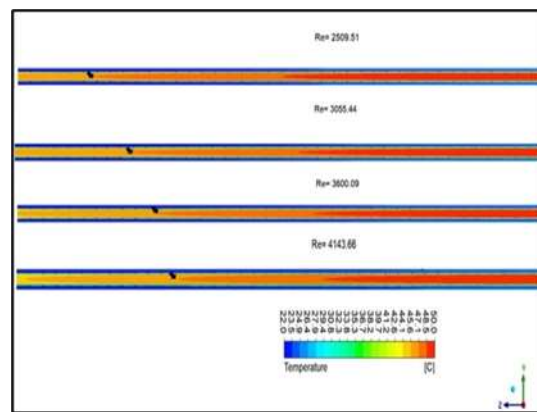
reliable basis for studying the impact of various geometric modifications on heat transfer performance. The **Figure(6)** illustrates the accuracy of the numerical model.



Figure(6) variation of Nusselt number with Reynolds number for smooth tube.

2.2 Temperature Field

Figure(7) presents the temperature field distribution across three key regions of the heat exchanger: the cold water flowing through the shell side, the solid tube wall, and the hot water inside the tube. The results are shown for four different Reynolds numbers on the tube side, ranging from approximately 2509 to 4143. A clear trend can be observed: as the Reynolds number increases, the temperature of the fluid inside the tube decreases more rapidly along the flow direction. This behavior is expected, as higher Reynolds numbers correspond to greater flow velocities, which in turn reduce the residence time of the fluid. As the fluid moves faster, it has less time to absorb heat, leading to a lower outlet temperature despite an overall improvement in convective heat transfer. Interestingly, the total amount of heat transferred from the tube-side water to the shell-side water remains nearly the same across all cases. This is because the boundary conditions, including inlet temperatures and mass flow rates — are kept constant, and the outer surface of the shell is thermally insulated. As a result, any gains in heat transfer efficiency due to higher Reynolds numbers are reflected primarily in how the temperature is distributed within the system, rather than in the total energy exchanged. It's important to highlight that while increasing the Reynolds number can be beneficial from a thermal perspective, it also introduces mechanical challenges. One of the main drawbacks is the associated rise in pressure loss within the tubes. Higher velocities cause more friction and turbulence, leading to increased pumping power requirements. Therefore, the design of such systems must carefully balance heat transfer performance with hydraulic efficiency. This trade-off between thermal enhancement and energy cost is critical, particularly in large-scale or continuous-flow applications.

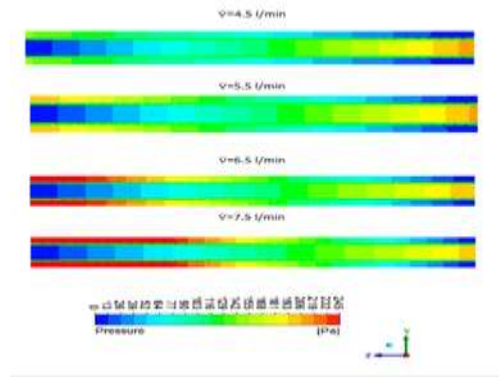


Figure(7) Temperature distribution of fluid and tube at different RE (2509-4143).

Pressure drop

Figure(8) illustrates the pressure distribution across the domain of the heat exchanger at different shell-side Reynolds numbers: 2509, 3055, 3600, and 4143. In all cases, the hot water flows through the inner tube at a constant flow rate of 3.5 L/min and an inlet temperature of 50°C. Meanwhile, the cold-water flows through the shell side at varying flow rates of 4.5, 5.5, 6.5, and 7.5 L/min, with an inlet temperature of 22°C. At the lowest shell-side Reynolds number (Re = 2509), the pressure drop is more dominant in the tube side, where the flow is faster. This is evident from the steeper pressure gradient along the tube compared to the shell. As the shell-side flow increases, the pressure field within the shell becomes more significant. For instance, at Re = 3055, the pressure drop in both the shell and the tube are approximately equal, reaching around 225 Pa. One interesting feature highlighted by the simulation results is the influence of the inner surface geometry of the shell. The pits along the shell wall appear to disturb the pressure field, creating noticeable local variations in the shell-side pressure distribution — a phenomenon that is not present in a smooth-walled configuration. This effect becomes more visible at higher Reynolds numbers. As the Reynolds number on the shell side continues to rise, the pressure drop increases accordingly. At Re = 3600, the pressure drop rises noticeably, and by Re = 4143.6, the shell-side pressure drop reaches approximately 405 Pa. This trend is consistent with the increase in flow rate and turbulence within the shell side, leading to higher frictional losses. These results have important design implications. The pressure drop in both the tube and shell sides directly affects the pumping requirements of the system. Higher pressure losses mean that more energy is needed to drive the fluid through the heat

exchanger, which influences pump sizing and overall system efficiency. As such, while optimizing thermal performance is critical, designers must also account for the hydraulic demands imposed by flow resistance, especially in applications involving structured or pits geometries.

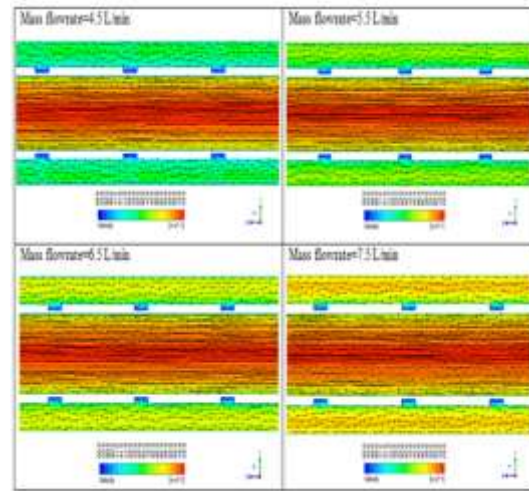


Figure(8) Variation of pressure field as Reynolds number of the shell changes.

2.3 Velocity Field

Figure 9 illustrates velocity vectors and contours for water flowing through a shell-and-tube heat exchanger with pits on the inner shell surface, designed to enhance heat transfer between the hot tube fluid and the colder shell fluid. The contours reveal higher velocities, up to 0.53 m/s, at the tube center, with shell-side THE FLOW RATE increasing from 4.5 to 7.5 L/min. The pits induce vortical flows, reducing local velocities but significantly boosting heat transfer by creating turbulence, aligning with recent studies showing such modifications disrupt the thermal boundary layer. This turbulence enhances the convective heat transfer coefficient, a critical factor in improving exchanger efficiency, as supported by research indicating Nusselt number increase in dimpled tube designs due to vortex formation. Turbulence and mixing are essential for optimizing shell-and-tube heat exchanger performance, promoting uniform temperature distribution and reducing thermal gradients that could lead to hotspots. Effective mixing, driven by perforations or baffles, minimizes boundary layer thickness, enhancing energy exchange, with studies showing a 17.4% increase in the heat transfer coefficient with optimized baffle designs. However, this comes with a trade-off, as turbulence can increase pressure drop by 20–60%, raising pumping costs, a challenge noted in recent papers on corrugated tubes. Optimizing perforation size and spacing could balance heat transfer gains with energy efficiency, making this design particularly

valuable for sustainable industrial applications like chemical processing, where energy recovery aligns with global green technology trends.



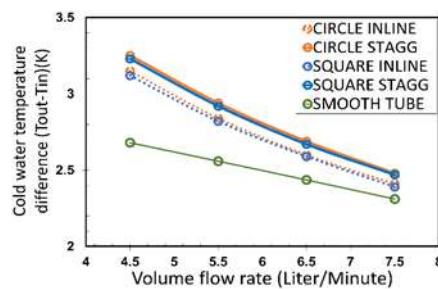
Figure(9) Velocity vector and contour of the fluid in shell and tube heat exchanger with pit on the internal surface of the shell

2.4 Effect of Pits

Figure 10 presents the variation in cold water temperature difference ($T_{out} - T_{in}$) with flow rate for various configurations of pit shapes and arrangements. As seen in the figure, a general trend across all cases is the decrease in the cold-water temperature difference with increasing flow rate. This behavior is in line with the principle of energy conservation. Since the rate of heat transfer (Q) in a heat exchanger is governed by the relation $Q = \dot{m} C_p \Delta T$, where \dot{m} is the mass flow rate, C_p is the specific heat capacity, and ΔT is the temperature difference across the exchanger. An increase in flow rate must be compensated by a decrease in ΔT when Q locally remains nearly constant and C_p experiences limited variation with temperature. It is evident, when comparing different configurations, that the inclusion of pits on the shell side significantly improves thermal performance relative to a smooth pipe. The highest improvement is observed with the circular pits in a staggered arrangement, achieving a temperature difference of up to 13% higher compared to the smooth tube at the same flow rates. This is followed by the staggered square configuration with an improvement of 12%, while the sequential circular configuration shows an increase of 10%, and the linear square configuration shows an increase of 9%. These enhancements can be attributed to the induced turbulence and secondary flows generated by the pit structures, especially when arranged in a staggered manner.

Such turbulence intensifies the mixing of cold water in shell side, disrupts the formation of the

thermal boundary layer, and increases the rate of convective heat transfer. The staggered arrangements, in particular, promote unsteady wake regions and flow separation behind pits, which further augment the local heat transfer coefficients. The smooth tube, in contrast, shows the lowest temperature difference across all flow rates. This confirms that in the absence of flow disturbance or turbulence-promoting features, the shell-side fluid tends to flow in a more laminar and stratified manner, leading to thicker thermal boundary layers and reduced heat transfer rates. The data clearly demonstrate the positive impact of using of circular or square pits, particularly in staggered patterns, is a promising passive enhancement technique for improving shell-side heat transfer. This insight can be valuable for the design of more compact and efficient heat exchangers in industrial applications.

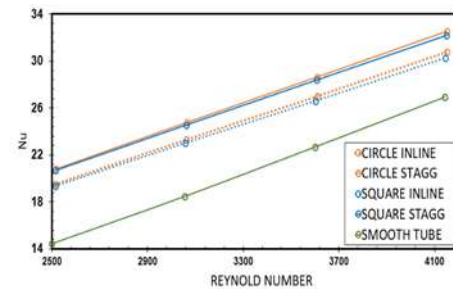


Figure(10) variation of temperature difference between inlet and outlet of cold water with flow rate.

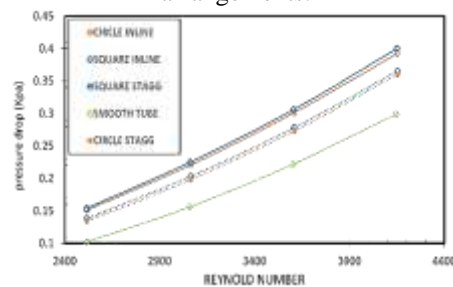
Nusselt number with Reynolds number for different pit geometries and arrangements on the shell side is illustrated in **Figure(11)**. As previously discussed in the temperature difference analysis, introducing pits on the internal surface of the shell significantly enhances thermal performance compared to a smooth tube. The Nusselt number and heat transfer coefficient increases with Reynolds number in all cases due to intensified turbulence. The circular staggered configuration consistently achieves the highest heat transfer coefficient, followed by the square staggered case, indicating that circular pits are more effective than square ones. Furthermore, staggered arrangements outperform inline ones because they promote greater flow disruption and mixing by preventing the formation of stable wake regions along the flow path. The smooth tube exhibits the lowest values, confirming the crucial role of induced turbulence in enhancing shell-side convection. These results affirm that pit-induced surface modifications improve heat exchanger effectiveness.

Figure(12) illustrates the relationship between Reynolds number and pressure drop. It is observed that

the pressure drop increases progressively with rising Reynolds number in all cases, which aligns with fluid dynamics principles. The smooth tube recorded the lowest pressure drop due to streamlined flow and the absence of internal disturbances. In contrast, the pits tubes exhibited a noticeable increase in pressure drop as a result of enhanced flow resistance and induced turbulence. Comparing the two arrangements, it is clear that the staggered configuration led to a higher pressure drop than the in-line configuration for the same pit shape. This is attributed to the greater flow disturbance caused by the staggered layout. Additionally, square pits generated a higher pressure drop than circular pits under the same arrangement, due to the sharper edges which obstruct the flow more than curved surfaces. Overall, the highest pressure drop was recorded for the square staggered case, while the lowest among the pits tube was observed in the circular inline configuration.



Figure(11) variation of heat transfer coefficient with Reynolds number for different pits shapes and arrangements.



Figure(12) variation of pressure drop with Reynolds number for different pits shapes and arrann

Conclusions

1-The numerical investigation demonstrated that the presence of pits on the shell side of the double-tube heat exchanger enhances turbulence intensity, which in turn improves heat transfer performance but also increases the hydraulic resistance, resulting in higher pumping power requirements. Among the tested configurations, the square staggered arrangement exhibited the highest pressure drop.

2-In terms of thermal performance, all pit geometries provided significant enhancement compared to the smooth tube. The maximum improvement in the average Nusselt number was achieved with the circular staggered configuration, recording an enhancement of 31%. This was followed by the square staggered configuration (30%), the circular inline configuration (24%), and the square inline configuration (22%).

3-These findings highlight that while pit-induced turbulence substantially boosts heat transfer, the associated pressure drop must be carefully considered. Therefore, an optimal heat exchanger design requires a trade-off between thermal enhancement and hydraulic efficiency to achieve balanced performance.

References

- [1] S.Kakac, H.Liu, and A.Pramuanjaroenkij, "Heat exchangers: selection, rating, and thermal design". CRC press, 2002
- [2] Malapur, H. V., Havaladar, S. N., & Kharade, U. V. (2022). Heat transfer enhancement of an internally and externally dimpled pipe heat exchanger–Numerical study. *Materials Today: Proceedings*, 63, 587-594.
- [3] Farsad, S., Mashayekhi, M., Zolfagharnasab, M. H., Lakhi, M., Farhani, F., Zareinia, K., & Okati, V. (2022). The effects of tube Dimples-Protrusions on the thermo-fluidic properties of turbulent forced-convection. *Case Studies in Thermal Engineering*, 35, 102033.
- [4] Vijayaragavan, B., Asok, S. P., & Shakthi Ganesh, C. R. (2023). Heat transfer characteristics of double pipe heat exchanger having externally enhanced inner pipe.
- [5] Ali, M. A., & Shehab, S. N. (2023). Numerical analysis of heat convection through a double-pipe heat exchanger: dimpled influence. *Journal of Engineering Research*, 11(1), 100016.
- [6] Ali, S. A., Barrak, E. S., Alrikaby, N. J., & Hameed, M. R. (2025). Numerical Study of Thermal-Hydraulic Performance of Forced Convection Heat Transfer in Dimple Surface Pipe with Different Shapes using Commercial CFD Code. *heat transfer*, 125(2), 1-15.
- [7] Cheng, J., Cheng, W., Lin, W., & Yu, J. (2024). Heat Transfer Performance and Flow Characteristics of Helical Baffle–Corrugated Tube Heat Exchanger. *Applied Sciences*, 14(19), 8905.
- [8] Mohammed, A. A., Mahmoud, M. S., Jebir, S. K., & Khudheyer, A. F. (2024). Numerical Investigation of Thermal Performance for Turbulent Water Flow through Dimpled Pipe. *CFD Letters*, 16(12), 97-112.
- [9] Ghashim, S. L. (2024). Flow field and heat transfer characteristics in dimple pipe with different shape of dimples. *Wasit Journal of Engineering Sciences*, 12(2), 125-136.
- [10] Zhang, Q., Shan, Y., Wang, N., Tian, Z., Liu, C., Wu, X., & Song, K. (2024). Numerical investigation on thermohydraulic characteristics in a circle tube with a novel arrangement of ellipsoidal dimples. *International Journal of Heat and Fluid Flow*, 110, 109631.
- [11] Al-Haidari, S. R., Mohammed, A., & Al-Obaidi, A. R. (2024). Analysis of thermal hydraulic flow and heat transfer augmentation in dimpled tubes based on experimental and CFD investigations. *International Journal of Heat and Fluid Flow*, 110, 109604.
- [12] Ali, S. A., Barrak, E. S., Alrikaby, N. J., & Hameed, M. R. (2025). Numerical Study of Thermal-Hydraulic Performance of Forced Convection Heat Transfer in Dimple Surface Pipe with Different Shapes using Commercial CFD Code. *heat transfer*, 125(2), 1-15.
- [13] Wantha, C. (2023). Heat transfer enancement in the annulus side of a double-tube heat exchanger using Al₂O₃-water nanofluids and dimpled outer tubes. *Heat and Mass Transfer*, 59(8), 1525-1542.
- [14] Hussein, H., & Freegah, B. (2023). Numerical and experimental investigation of the thermal performance of the double pipe-heat exchanger. *Heat and Mass Transfer*, 59(12), 2323-2341.
- [15] Marzouk, S. A., Almeahadi, F. A., Aljabr, A., & Sharaf, M. A. (2024). Numerical and experimental investigation of heat transfer enhancement in double tube heat exchanger using nail rod inserts. *Scientific Reports*, 14(1), 9637.
- [16] Somanchi, Naga Sarada, Gugulothu, Ravi and Tejeswar, S. V. (2024). Experimental investigations on heat transfer enhancement in a double pipe heat exchanger using hybrid nanofluids. *Energy Harvesting and Systems*, vol. 11, no. 1, pp. 20230065.